Cement & Concrete Composites 31 (2009) 153–162

Contents lists available at ScienceDirect

Cement & Concrete Composites

journal homepage: www.elsevier.com/locate/cemconcomp

Interaction of polycarboxylate-based superplasticizers with cements containing different C_3A amounts

Anatol Zingg [a,*], Frank Winnefeld [a], Lorenz Holzer [a], Joachim Pakusch [b], Stefan Becker [b], Renato Figi [a], Ludwig Gauckler [c]

[a] Empa, Swiss Federal Laboratories for Materials Testing and Research, Laboratory for Concrete/Construction Chemistry, Ueberlandstrasse 129, 8600 Duebendorf, Switzerland
[b] BASF AG, GKD/C-B1, Carl-Bosch-Strasse 38, 67056 Ludwigshafen, Germany
[c] ETH, Swiss Federal Institute of Technology Zurich, Institute of Nonmetallic Inorganic Materials, Department Materials, Wolfgang-Pauli-Strasse 10, 8093 Zurich, Switzerland

ARTICLE INFO

Article history:
Received 19 February 2008
Received in revised form 2 January 2009
Accepted 7 January 2009
Available online 20 January 2009

Keywords:
Superplasticizers
Zeta potential
Adsorption
Rheology
Cement
C3A-content

ABSTRACT

This parametric study links the molecular structure of a carboxylate-type of superplasticizer with their performance in cement pastes with different C_3A-contents. Beside the variation of the C_3A-content, the experimental synthesized superplasticizers have been varied by polyethylene-oxide side chain density and length. The connection between the superplasticizers, their effect on workability properties and retardation phenomenon and the dependency of C_3A-content in the cement paste has been investigated.

The characteristic interaction phenomenons between different PCE-architectures and different C_3A-contents have been examined by calorimetric, rheological, adsorption, and zeta potential measurements. This study shows that with decreasing side chain density the PCE molecules adsorb stronger and thus, lower the yield stress of a cement paste by steric stabilization. It is also shown that PCE molecules with long side chains delaying the setting of the cement paste to less extend than PCE molecules with shorter side chains. Consequently, in terms of optimization of the molecular architecture, good workability can be achieved by addition of highly charged PCE with long side chains. The latter minimizes undesired retardation phenomena.

1. Introduction

Superplasticizers are frequently used in concrete technology in order to improve the workability of mortar and concrete systems for demanding applications. The addition of superplasticizers is aiming at two objectives: first, the addition of superplasticizers allows controlling the flow properties, which are of major importance for the design of, e.g., self-compacting concretes, and second, superplasticizers allow the reduction of the water to cement ratio while maintaining workability in order to reach high strength and durability.

The properties of cement–water systems are depending on various chemical and physical parameters. The precipitation of hydrate phases during early hydration (up to 3 h until setting) and thus workability are affected on one hand by the chemical composition of the clinker, essentially its C_3A-content, the availability of soluble sulphates and the chemical composition of the pore solution. On the other hand, physical properties such as particle size distribution, packing density, surface area and the interparticle forces govern the rheological behaviour of cement pastes.

The cement–water system is highly sensitive to the addition of superplasticizers. Already small amounts of superplasticizers enhance the workability properties efficiently, but are often associated with strong, undesired retardation phenomena of the setting of the cement paste.

Newer superplasticizer generations are based on comb-shaped polycarboxylates (as used in this study, hereinafter called PCE). Their dispersing effect is due to the adsorption of polymers on particle surfaces and evocation of electrostatic and/or steric repulsive forces [1,2]. Those mechanisms can be derived from theories of colloidal sciences [3–5].

The addition of superplasticizers impacts the interface between particle surface and the pore solution and influences physical properties such as viscosity and yield stress of the paste. The adsorption behaviour depends on the PCE architectures. The molecules are comb-shaped, consisting of an adsorptive backbone unit and a hydrophilic polyethylene-oxide (PEO) side chain [6]. Both parameter, side chain length and side chain density, can be varied in order to take control of the adsorption behaviour and dispersion ability.

By changing PCE architecture and dosage, workability properties and prolongation of the dormant period can be controlled [7–11]. Despite numerous research project have been carried out

* Corresponding author. Present address: Holcim Group Support Ltd., Im Schachen, 5113 Holderbank AG, Aargau, Switzerland.
E-mail address: azingg@postmail.ch (A. Zingg).

0958-9465/$ - see front matter © 2009 Elsevier Ltd. All rights reserved.
doi:10.1016/j.cemconcomp.2009.01.005

on the subject cement–superplasticizer interaction, many questions remain unsolved. Certain cement–superplasticizer combinations are incompatible [12–14] exhibiting poor flow behaviour, early slump loss, strong retardation or flash set.

The study presented here is part of a project where macroscopic phenomena of cementitious suspensions containing superplasticizers [15–17] are linked to their microstructural evolution [18,19] during early hydration up to setting. This paper aims to contribute to a better understanding of the interaction mechanisms of PCE with cement of different C_3A-contents (all cements are CEM I 42.5 N types) in fresh cement pastes. In this parametric study, the PCE-architecture (side chain density, side chain length) and the C_3A-content of cement are systematically varied.

The interaction between cement and superplasticizers is investigated using isothermal calorimetry, rheology measurements, TOC anaylsis and zeta potential measurements. Adsorption data are gained in order to quantify the amount of superplasticizer involved in the electrostatic and/or steric stabilization of a fresh cement paste. The impact of adsorbed PCE on the interparticle forces is followed by recording the zeta potential of the cement pastes. Rheological and calorimetric measurements are carried out in order to get a better understanding for the paste rheology and for the heat of hydration evolution for each cement–superplasticizer couple.

2. Materials

2.1. Superplasticizers

For this study, three comb-shaped polycaboxylate-type superplasticizers (PCE) were synthesized. Methylpolyethyleneglycol copolymers (side chains) were grafted on a methacrylic acid copolymer (backbone). The polymer architecture is varied by using different side chain densities and lengths. The chemical structure is shown in Fig. 1.

The PCEs were synthesized as follows: preformation of mono unsaturated "teeth" and linking of (meth)acrylic acid units with alkyl-polyethylene glycols followed by radical copolymerization with additional (meth)acrylic acids as described in Winnefeld et al. [15]. In order to ensure the same reaction kinetics, the molar concentrations of all monomers were kept constant during the polymerization which leads to different final solid contents of the products. This circumstance was compensated in all paste and mortar tests by referring to the dry matter of the admixture and correcting the water/cement ratio by the water content of the polymer solution. However, for certain data comparisons of the different polymer architectures, it is useful to refer to the charge density (mol carboxylic acid groups per gram cement). The used PCE architectures and their molecular characteristics as well as their calculated (theoretical) charge densities are listed in Table 1. Generally, the charge density increases with lower side chain density and shorter side chain length (charge density PCE 23-6 > PCE 102-6 > PCE 102-2). All superplasticizers were applied as sodium salts.

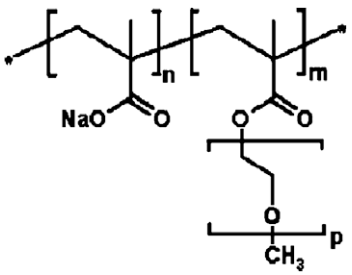

Fig. 1. Chemical structure of the experimental superplasticizers (copolymers of methylpolyethyleneglycol-methacrylate and methacrylic acid, sodium salts) with back bone (n) to side chain (m) unit ratio of n:m = 2:1, and 6:1; number of PEO units (p) in the side chains: p = 23 and 102.

2.2. Portland cements

Three ordinary Portland cements (CEM I 42.5 N) according to European Standard EN 197-1 have been used for this study (Table 2). According to Bogue calculations (Table 3), these cements exhibit C_3A-contents of 1% (L-OPC), 8% (M-OPC), and 10% (H-OPC) respectively. The cements also differ in their Al_2O_3/SO_3 ratio (1.9, 1.7, and 2.1, respectively). Their specific surfaces (Blaine values) range within 3000–3600 cm^2/g.

3. Sample preparations and methods

In order to compare the results obtained from different measurement methods, water to cement ratio of 0.35, hydration times and PCE concentrations were kept constant. Variations will be mentioned in the relevant sections. For all measurements, except for the zeta potential titration experiments, simultaneous addition of PCE was applied. The PCE solutions and water were premixed whereas for the zeta potential measurements the PCE was titrated after mixing the cements with water.

3.1. Conduction calorimetry

All experiments were carried out using an isothermal heat flow calorimeter (Thermometric TAM Air) at a measurement temperature of 20 °C. For each sample 6.00 g of cement were weighted into a flask and 2.10 ml of water or water-admixture solution (0.10%, 0.20%, and 0.30% of cement weight) were added. The cement paste was then mixed with a small stirrer for 2 min. Afterwards, the flask was capped and placed into the calorimeter. Note that the initial heat peak is not recorded due to external mixing. The heat flow was recorded for 72 h.

The onset of the acceleration period was derived from the calorimetric curve in two steps: first, determination of minimum heat flow during the dormant period, second, addition of 0.25 J/(g h) to the determined minimum value. The hydration time reached at the onset of each cement–superplasticizer couple is then defined as the starting time of the acceleration period. The value of the starting time of the acceleration period (as described above) determined from the heat flow curve roughly corresponds to the "initial setting" determined by the Vicat needle test (according to European Standard EN 196-3) given in Table 2. Hereinafter, the term "setting time" is used for the determined start of the acceleration period from the heat flux curve.

3.2. Rheology

A kitchen blender (Brown Multiquick 5550 M CA) was used for mixing. All cement pastes were prepared by weighting 300 g of cement into the mixing bowl and by adding 105 g of water or water-admixture solution (0.05%, 010%, 0.15%, and 0.20% of cement weight). The mixing procedure was set to 60 s of mixing at stage 6, 30 s scraping the paste off the walls of the bowl by hand and then again 60 s of mixing at the same stage. A Paar Physica MCR 300 rheometer with concentric cylindrical geometry was used for these experiments. The rotating bob was serrated with 100 μm deep vertical lines. The gap between the rotating bob and the cylindrical beaker was 1.13 mm with a ratio between outer and inner cylinder of 1.08. The temperature of the cement paste was controlled by a water bath and kept at 20 °C.

Table 1
Characterization of the polycarboxylate-ether superplasticizers.

Polymer	Length of side chain p	Density of side chains n:m	M_n[a] (g/mol)	M_w[b] (g/mol)	PDI[c] (M_w/M_n)	Solid content mass (%)	Mol anionic sites[d] (g PCE)
PCE 23-6	23	6:1	7600	18,900	2.5	13.8	$3.4 \times 10-3$
PCE 102-2	102	2:1	16,800	78,000	4.7	46.3	4.2×10^{-4}
PCE 102-6	102	6:1	14,600	67,000	4.6	21.0	1.1×10^{-3}

[a] M_n = number-average molecular weight.
[b] M_w = mass-average molecular weight.
[c] PDI = M_n/M_w = polydispersity index.
[d] Calculated values.

Table 2
Chemical composition and calculated properties of the used ordinary Portland cements CEM I 42.5 N.

	CaO (wt.-%)	MgO (wt.-%)	SiO_2 (wt.-%)	Al_2O_3 (wt.-%)	Fe_2O_3 (wt.-%)	Na_2O (wt.-%)	K_2O (wt.-%)	SO_3 (wt.-%)	CO_2 (wt.-%)	LOI[a] (wt.-%)	Free lime (wt.-%)	Sp. surf. (cm^2/g)	Vicat setting time (min)
L-OPC	61.2	1.8	18.7	4.3	6.2	0.13	1.0	2.3	2.56	2.75	0.47	3560	235
M-OPC	63.4	1.8	20.0	4.8	2.5	0.10	0.94	2.8	1.85	2.29	0.76	3150	200
H-OPC	61.8	2.1	19.2	5.4	2.8	0.33	0.95	2.6	2.79	3.35	1.14	3090	185

[a] Loss on ignition.

Table 3
Mineral composition after Bogue, calculated from XRF-data.

	C_3S (wt.-%)	C_2S (wt.-%)	C_3A (wt.-%)	C_4AF (wt.-%)	$CaSO_4$ (wt.-%)	K_2SO_4 (wt.-%)	Na_2SO_4 (wt.-%)	CaO (wt.-%)	$CaCO_3$ (wt.-%)
L-OPC	54	15	1	20	2.5	1.6	0.1	0.5	5.8
M-OPC	57	16	8	8	3.1	1.7	0.1	0.8	4.2
H-OPC	54	17	10	9	2.8	1.5	0.3	1.1	4.0

After blending, the cement paste was transferred into the measurement beaker by a spoon. Then, the measuring system with a rotating bob was lowered to measuring position and the beaker was covered with a solvent trap to protect the sample from water evaporation. The measurements were taken 5, 30, and 60 min after blending performing 1 min pre-shearing at a shear rate of 100 s^{-1} in order to break particle agglomerates. Afterwards, a flow curve with shear rates between 100 and 0.1 s^{-1} was recorded using a ramp time of 5 s in the shear rate range of 100–1 s^{-1} and of 10 s for shear rates below 1 s^{-1}. Apparent yield stress and plastic viscosity were calculated using the Bingham model.

3.3. Adsorption isotherms

To determine the superplasticizer adsorption isotherms, the same blending procedure as for the rheology samples was used. 5, 30, and 60 min after mixing, the alkaline pore solution was removed through a 0.45 μm Nylon filter by air pressure filtration. 1 ml of the solid free pore solution was then stabilized by adding 9 ml of 0.1 mol/l HCl. The total organic content (TOC) of the pore solution samples were then determined by using a Shimadzu TOC-Analyzer 5000 A. The consumed amount of PCE was calculated from reference TOC measurements of aqueous polymer solutions.

In order to correct the adsorption measurements for the organic content of the Portland cements due to e.g., grinding agents, TOC of pore solutions of plain cement pastes were taken as well. In addition, the TOC content of the used deionized water was measured. Both background values were taken into account when calculating the consumed amounts of PCE.

3.4. Zeta potential

All zeta potential data were collected with the ZetaProbe (Colloidal Dynamics Inc.), which works on the basis of the electroacoustic method. A high frequency alternating electric field is applied and causes charged particles to oscillate. The motion of the particles generates a sound wave which is recorded and delivers the dynamic mobility of the suspended particles. The software calculates the zeta potential from the dynamic mobility.

Foregoing the sample measurements, pH-meter (4.01, 7.01, and 10.01) and zeta dip probe (KSiW-standard, provided by Colloidal Dynamics Inc.) were calibrated. All samples were measured in a beaker and stirred (400 rpm) in order to prevent segregation. The syringe-unit (titration unit) was washed prior to the use with the titrant to insure its purity.

All cement pastes were blended using same procedure as for the TOC and rheology experiments. Approximately 270 ml of cement paste (beaker weighted empty and filled with cement paste for later corrections) was then transferred into the beaker. In a preliminary test series, all cement pastes used for this study were found to yield a stable zeta potential after 15 min of hydration.

For the investigation of the impact of PCEs with different architectures on the zeta potential of the cement paste, concentration series with constant titration increments of diluted PCE solution of 0.025 weight percentages referring to cement were measured. This experimental setup measures the impact of delayed PCE addition.

The obtained raw data of for the zeta potential are strongly affected by the fact that the pore solutions of cement pastes are highly charged with various ionic species and charged polymer. Therefore, background measurements were carried out using the following procedure: first, pore solutions of each cement paste was extracted by air pressure filtration and then diluted until the conductivity of the cement paste after 15 min (~15–25 mS/cm) was reached. Second, background measurements of different conductivity levels from 15 to 25 mS/cm (increment of 1 mS/cm) were measured because the conductivity of cement pastes increases with time. Third, PCE was titrated to a 18 mS/cm pore solution. After each titration step a background measurement was taken. Subsequent to each experiment, the raw data collected by the ZetaProbe was recalculated by applying the corresponding conductivity/PCE

titration background files (taken for each titration step as described above).

4. Results and discussion

4.1. Conduction calorimetry

The heat evolution of cement pastes depends on one hand on the mineralogical composition and on the other hand on physical parameters such as fineness and particle size distribution of the cement. At this early stage of hydration, the C_3A-content and the availability of sulphates which determines type and amount of hydration products, is a key factor. The total hydration reactions can be followed by recording the heat flow of the cement paste.

Directly after addition of water to the cement, a part of the C_3A dissolves quickly. This leads to formation of ettringite if sufficient sulphate ions are provided [20]. Otherwise, flash setting of the cement paste could occur. It has to be kept in mind that this study uses commercial available cements and therefore, their sulphate contents had been adjusted in order to prevent flash setting. Furthermore, the setting times for all three cements ranges from 185 (H-OPC) to 235 (L-OPC) minutes (Table 3) and are within the requirements of European standard EN 197-1.

The heat flow curves of the three cement pastes exhibiting different C_3A-contents are shown in Fig. 2. Higher C_3A-contents result in higher heat release during the dormant period. This higher heat flow indicates an exothermal process, which may be related to increased formation of ettringite. The main hydration peak of H-OPC is broader and the peak height is lower than for L-OPC and M-OPC. Due to the high amount of Al_2O_3 in the cement, in H-OPC cement pastes the sulphate is probably earlier exhausted than in L-OPC and M-OPC cement pastes. According to the literature [21–24], the right part of the peak can be assigned probably to the so-called sulphate depletion peak. C_3S hydration (probably left part of the peak) and sulphate depletion peak do overlap less in H-OPC paste compared to M-OPC and L-OPC.

The presence of PCE generally shows some retarding effect on the start of the acceleration period of cement pastes. The higher the charge density of a PCE (Fig. 3, left column) and the higher the PCE dosage (Fig. 3, right column), the stronger the setting is delayed. With increasing contents of C_3A in the cement pastes the retardation effect of the PCEs decreases independent of their architecture and dosage (Fig. 3, increasing C_3A-content from top to bottom).

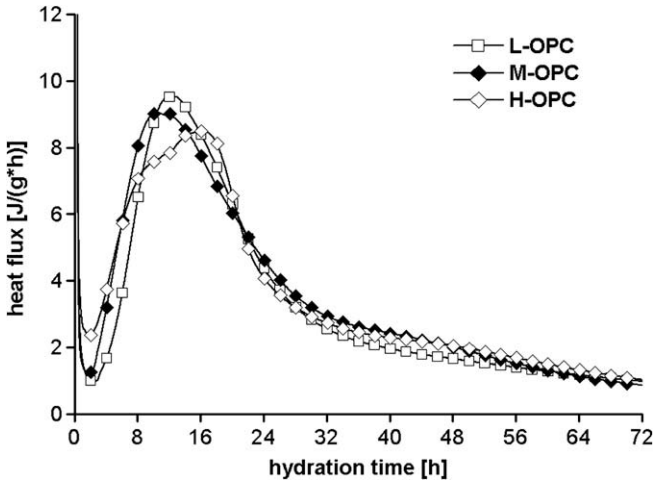

Fig. 2. Conduction calorimetry curves: heat flows of L-OPC, M-OPC and H-OPC cement pastes with w/c 0.35 measured for 72 h. The noted setting times are set equal to the start of the acceleration period.

Generally, PCE 102-2 shows the smallest influence on the cement pastes concerning the delay of the onset of the acceleration period (Fig. 3, left column). Even at higher concentrations, PCE 102-2 does hardly retard the onset of the acceleration period and does not influence the main hydration peak shape. This indicates no or only little interaction between the PCE molecules and the mineral phases of the cement paste (i.e. adsorption), because (i) the charge density is low (high side chain density) and (ii) the high side chain length allows only poor accessibility to the anionic sites of PCE 102-2 and thus, adsorption is hindered.

Generally, the presence of higher charged PCE (23-6 and 102-6) lead to a shift of the main hydration peak to the right and thus delays the acceleration period of the cement paste (L-OPC and M-OPC). Decreasing side chain density (PCE 102-6 < PCE 102-2) and shorter side chains (PCE 23-6 < PCE 102-6) prolong the setting times, whereas the latter effect is more pronounced. Similar results are reported by other authors [8,10]. Generally it is assumed, that PCE molecules preferably adsorb on C_3A, C_4AF and their hydration products. However, they mainly retard C_3S hydration [16,25,26], thus delaying the formation of C–S–H and portlandite. These findings are supported by TGA data taken from Winnefeld et al. [16] in Fig. 4 where the formation of portlandite starts after 4 h in a M-OPC paste (w/c = 0.35) without PCE (start of acceleration period) whereas with 0.2 wt.-% PCE 23-6 (system still in dormant period) no portlandite is formed at this time. The formation of portlandite in the paste (w/c = 0.35) with PCE starts after 18 h (start of acceleration period). No significant difference between the amounts of portlandite in the two pastes could be observed after 28 days. In addition, no delay of ettringite formation nor significant differences in the amount of ettringite precipitated was observed.

The presence of highly charged PCE (23-6 and 102-6) not only shift the main hydration peak of H-OPC cement pastes (Fig. 3, right figure bottom row) but also changes the peak shape. The peaks are the sum of simultaneous ongoing hydration processes of different clinker phases and thus, interpretations of peak shape and its changes in presence of PCE are difficult. However, even at low concentrations of PCE 102-6 (almost no retardation) the shape of the main hydration peak is narrower and its intensity higher.

One mechanism could be a simple peak shift in presence of PCE, where the C_3S hydration peak and the sulphate depletion peak completely overlap. A shift of the sulphate depletion peak to the left would imply earlier exhaust of sulphate and thus implies that in presence of PCE 23-6 and PCE 102-6, the renewal of C_3A hydration would occur earlier and roughly at the same time as the C_3S hydration. Consequently, in presence of high charged PCE, the consumption of sulphate must be increased. Other studies have measured increased amount of monosulphate and suggest a so-called orangomineral phase in presence of PCE [27,28]. However, it is not clear, how and to what extend the available amount and concentration of sulphate ions are influenced by the formation of such organomineral phases or vice versa. Another study by Peng [29] has shown, that PCE molecules can be adsorbed on gypsum surfaces as well. One could hypothesize, that the early formation of monosulphate phases are not due to intercalation of organomineral phases but due to hindrance of dissolution of sulphate of PCE-coated sulphate phases and thus, decreased availability of sulphate.

Another mechanism could be a shift of the sulphate depletion in presence of PCE 23-6 and PCE 102-6 to the right, indicated by the shoulder after the main hydration peak. This could be due to competitive adsorption between sulphate ions and the carboxylic groups of the PCE molecules during initial hydration [30,31]. Partial (or total) replacement of sulphate by PCE molecules in the double layer leads to less sulphate consumption and thus would ensure a sufficient supply of sulphate ions during the acceleration period and main hydration later on. This hypothesis fits well the

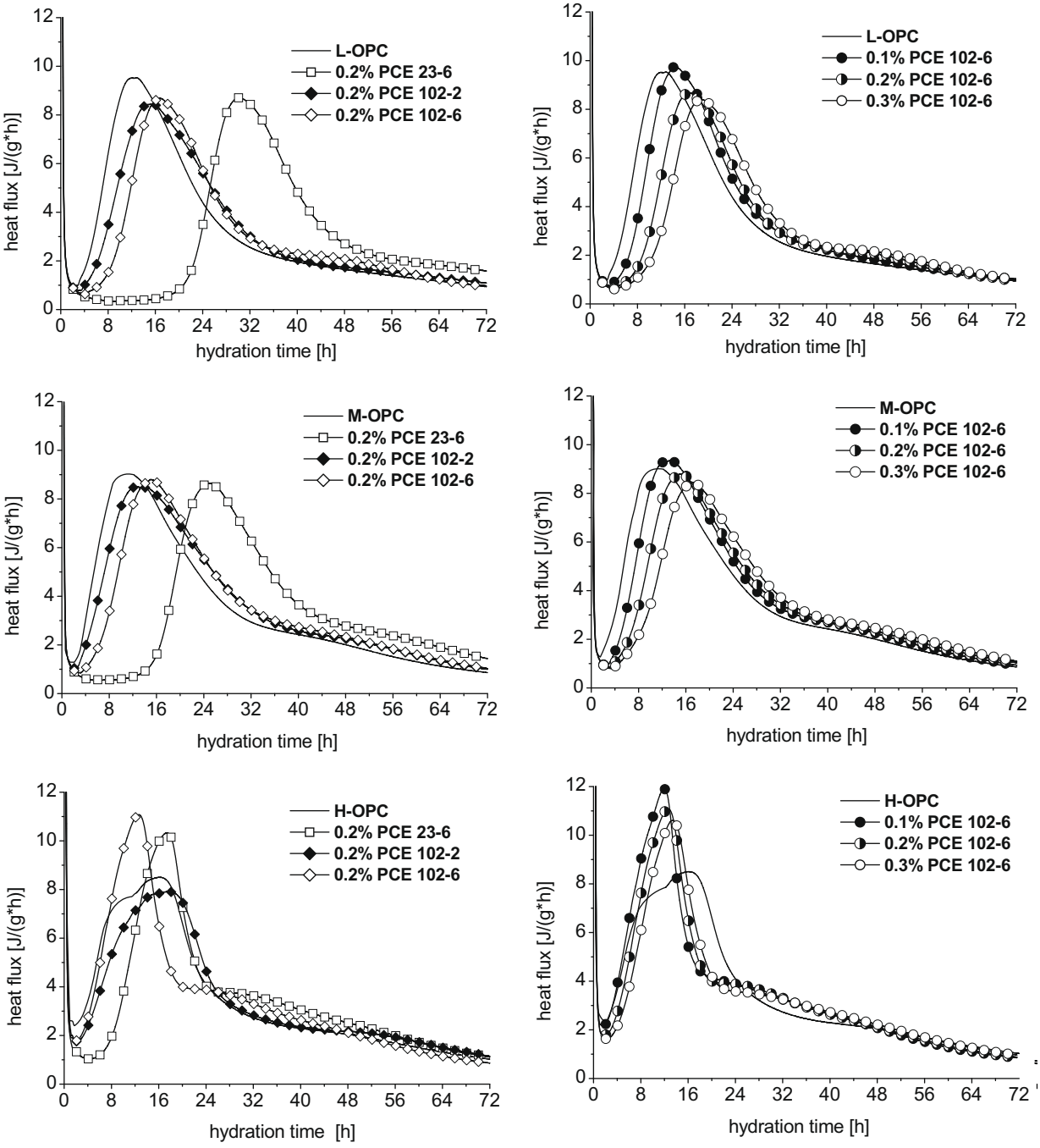

Fig. 3. Conduction calorimetry curves: heat flow of cement pastes with w/c 0.35 measured for 72 h. The C_3A-contents of the cements increase from top to bottom row. The left column shows the influence of PCE architecture; the right column shows the influence of dosage (PCE 102-6).

presented result obtained from calorimetry where the shoulder after the main hydration peak may indicate the remnant of the sulphate depletion peak.

4.2. Rheology

In this study, apparent yield stresses of cement pastes after 5, 30, and 60 min of hydration were measured. This paper reports only the 5 min data because all samples show only slight increases of yield stress within the first 60 min.

The apparent yield stresses of plain L-OPC and M-OPC pastes are about 30 Pa whereas for the H-OPC a significantly higher (55 Pa) yield stress was measured (Fig. 5, C_3A-content increases from top to bottom). Due to its C_3A-content [32] the latter cement system produces higher amounts of ettringite. The formation of ettringite consumes a reasonable amount of water and thus, the volume of free pore solution is reduced, while the solid content increases.

Independent of the C_3A-content of the cement it turned out, that a low charge density PCE (high side chain density and long side chains) hardly affects the yield stress of the cement paste. Despite long polyethylene-oxide side chains are thought to increase the paste fluidity by steric repulsive forces [1,8,33], the combination with a high side chain density seem to prevent PCE adsorption and thus, steric stabilization of the paste. With increasing charge densities, the fluidization ability of the PCE improves significantly. Above a certain side chain density (around 4:1), the influence of

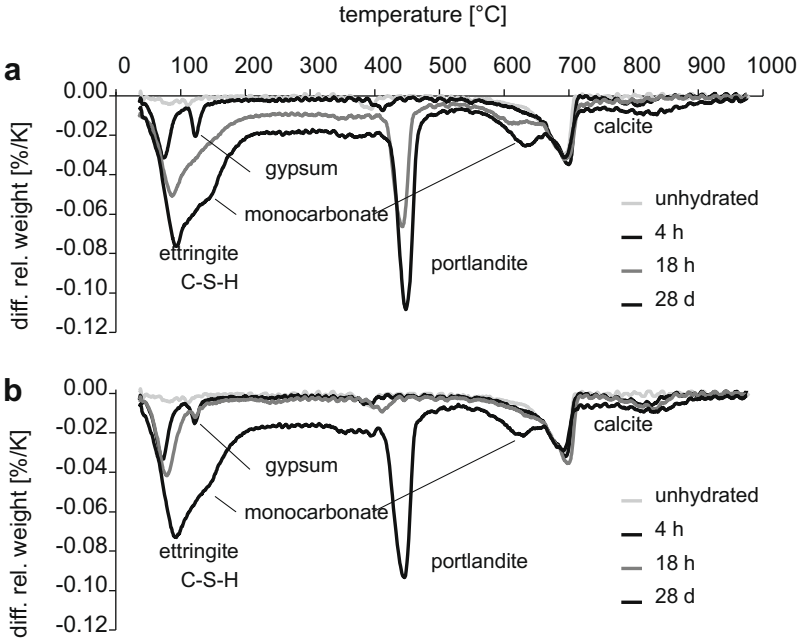

Fig. 4. Differential thermogravimetric analysis of medium C_3A-content OPC pastes (M-OPC) with w/c 0.35 after 0, 4, 18 h and 28 days of hydration time. M-OPC paste without superplasticizer (a); M-OPC paste containing 0.2% of PCE 23-6 (b).

the side chain length was found to be negligible in a previous study [15,16]. Both, PCE 23-6 and PCE 102-6 are capable to lower apparent yield stress already at low concentrations (Fig. 5). However, an increased PCE 102-6 concentration leads to bleeding phenomenon at lower concentrations than PCE 23-6 does. This observation is supported by slump flow measurements on mortars (unpublished results) where PCE 102-6 shows better flow behaviour than PCE 23-6 does. In addition, Fig. 6 shows that with same charge density, PCE 102-6 decreases the yield stress more efficiently than PCE 23-6. Remember, in this study the backbones of all PCEs were kept roughly at constant lengths. Therefore, in terms of charge densities, the comparison of the yield stress values referred to mol anionic sites of the PCE (mol anionic sites/g cement) is much more reasonable. After Plank et al. [31], the carbon bonds of the side chains of polycarboxylates have high rotational degrees of freedom. Therefore, it can be assumed, that PCE 23-6 and PCE 102-6 molecules have the same adsorption abilities but differ in their potential for steric repulsion, where PCE 102-6 with longer side chains is more efficient.

4.3. Adsorption of PCE

No significant differences in the adsorption isotherms after 5, 30, and 60 min have been found. This indicates a rapid PCE adsorption process shortly after contact of the cement powder with water. Assuming that polyethylene-oxide side chains are very flexible, the backbone charge density should be the decisive parameter which mainly determines the adsorption ability of a PCE molecule. In addition, a previous study on similar cement–water–superplasticizers systems revealed, that the PCE fraction with the higher molecular weight is adsorbed preferably [15,34].

Increasing C_3A-content of the cement leads to higher PCE adsorption (Fig. 7, C_3A-content increases from top to bottom) and requires higher PCE concentrations in order to reach saturation. This may be an indication of preferred PCE adsorption on aluminate phases, which is supported by a study of Yoshioka [35]. They carried out their investigation on pure clinker phases and could show a preferred PCE adsorption on C_3A and C_4AF and their hydration products.

Independent of the C_3A content of the cement paste, PCE 102-2 (high side chain density and high side chain length, low charge density) does hardly adsorb. This result fits well the obtained yield stresses of the same cement pastes, where PCE 102-2 shows only minor influenced on paste rheology. It can be concluded, despite the very flexible carbon bonds of the PEO side chains [31], that the accessibility of the carboxyl-groups for PCE with high side chain density is hindered and thus, strong adsorption such as ionic binding is not possible. With increasing side chain length and density, the carboxyl equivalents (mol carboxyl groups/g PCE) increase and thus, lead to lower the charge densities.

Generally, the PCE adsorb increasingly with decreasing side chain density. Above a ratio of four backbone units to one side chain unit [15], the influence of side chain length seems to be negligible (Fig. 7) as shown in e previous study. The graph of PCE 23-6 is congruent with the one of PCE 102-6. However, if the charge densities are compared, PCE 102-6 reaches saturation at a lower adsorbed carboxyl groups. This might be due to the fact, that the steric action radii of the longer side chains of PCE 102-6 are larger than PCE 23-6 and thus, less molecules are needed in order to reach the same fluidization state. Despite lower saturation concentrations the efficiency of the larger PEO side chains seems to have stronger influences on the workability of a cement paste. This can be attributed to higher steric repulsive forces of the longer PEO side chains.

However, by TOC analysis of the pore solution, the amount of PCE adsorbed on cement and hydrate particles is measured indirectly and may not represent the actual amount of PCE adsorbed. According to Flatt and Houst [28], the term ‘‘consumption” should be used rather than ‘‘adsorption” because adsorbed PCE and intercalated PCE can not be distinguished. However, PCE coprecipitation with mineral phases (e.g. monosulfate, monocarbonate) and thus the formation of organomineral-phases, may act as a chemical sink for PCE molecules. According to Plank et al. [27], PCE with short side chain length shows higher affinity for intercalation and thus, formation of organomineral phases. Intercalation counteracts the

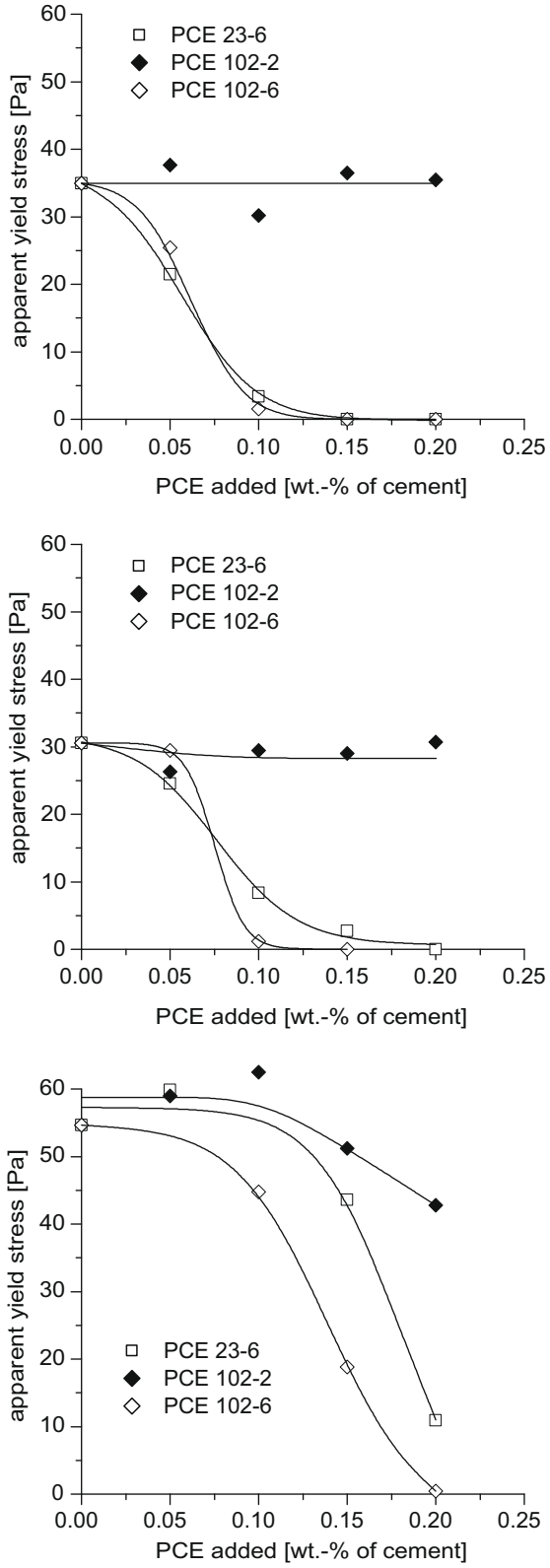

Fig. 5. Apparent yield stresses (Bingham model) measured on cement pastes with w/c 0.35 containing PCE (0.00%, 0.05%, 010%, 0.15%, and 0.20% weight of cement) after 5 min of hydration. The C_3A-contents of the cements increase from top to bottom row.

dispersion ability of the PCE. This is especially the case for cements where a high level of C_3A is combined with insufficient supply of sulphate (high Al_2O_3/SO_3 ratios) during early hydration.

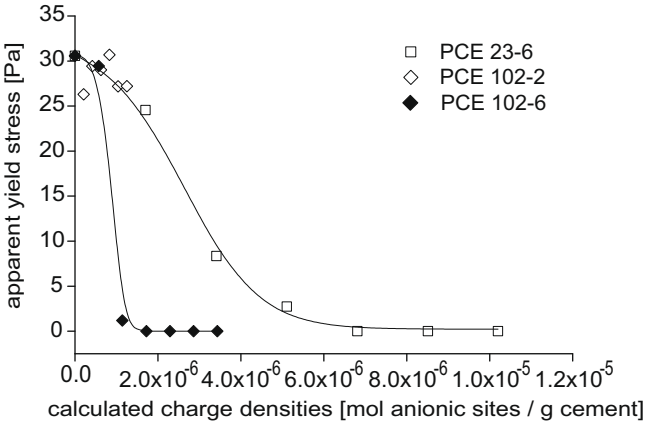

Fig. 6. Apparent yield stresses of M-OPC pastes with w/c 0.35 versus calculated charge densities (mol anionic site/g PCE) of PCE after 5 min of hydration from 0.00% to 0.30% in 0.05% steps.

4.4. Zeta potential

Dealing with cement–superplasticizer interaction phenomenons, the question about the relevant interparticle forces is of major importance. Surface charges and the availability of ionic species (counter-ions) and thus the constitution of the diffuse double layer determine the behaviour of two approaching particles. The zeta potential represents the potential at the slip surface where a particle in motion separates from the surrounding liquid phase. It is the potential that an approaching particle "feels".

After (initial period) 15 min, all cement pastes reach an "apparent" steady state with zeta potentials between −5 and −7 mV (Fig. 8, C_3A-content increases from top to bottom). Those zeta potentials are in good agreement with values reported in literature [5,36]. The negative zeta potentials are probably due to negative zeta potential of C_3S and C_2S [35] as the major components in the cement. But this is discussed controversially in literature where for the C_3S also positive zeta potentials [17,37–39] are given. Other studies report positive zeta potentials [40,41] or both, negative and positive zeta potentials [3,42] for cement pastes. However, the cements used in those papers differ in their mineralogical composition, the reactivity of their components and thus, in composition of their pore solutions. Note that often publications lack precise information about the experimental setup and sample parameters used and thus, direct comparisons of the data are difficult.

In this study, the zeta potentials for the plain cement pastes are found to be stable between 15 and 60 min of hydration, independent of the C_3A-content. After 60 min a slight increase of around 2–4 mV could be observed. This may result in a stronger flocculation of the cement paste which is in agreement with the slight increase of its yield stress and viscosity. The slow but still ongoing formation of ettringite during the dormant period could be an explanation for this behaviour.

In contrast to the stable zeta potential of cement pastes, their conductivity increases with evolving hydration time and is mainly influenced by dissolution, formation of hydrate phases and thus, evolution of solid content. Throughout preliminary titration studies, cement pastes consistently showed lower increase of conductivity with increasing PCE contents (Fig. 8). This fact may indicate either complexation of cations by anionic PCE molecules or slowed dissolution caused by adsorption and coverage of PCE molecules on clinker surfaces. The latter may act as diffusion barriers and lowering the surface area of C_3A directly connected with the pore solution. Other investigations have found the complexiation to be negligible as the chemical composition of the pore solution evolves independent of PCE presence [25] or have found complexes with

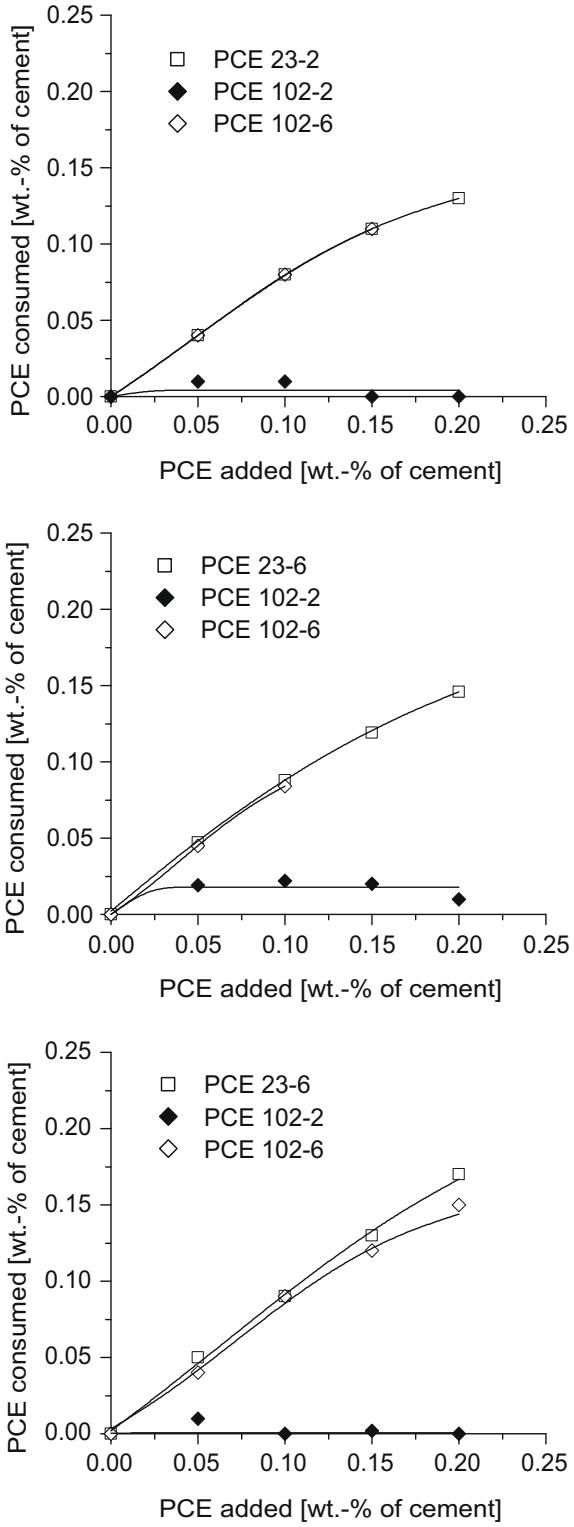

Fig. 7. Adsorption isotherms (obtained from TOC analysis) of cement pastes are shown with w/c 0.35 containing PCE (0.00%, 0.05%, 010%, 0.15%, and 0.20% weight of cement) after 5 min of hydration. The C_3A-contents of the cements increase from top to bottom row.

calcium ions exhibiting only low stability constants [43]. Therefore, the mechanism of PCE adsorption and formation of diffusion barriers is favoured.

The titration of cement pastes with higher charged PCE 23-6 and PCE 102-6 leads to a zeta potential shift close to zero charge

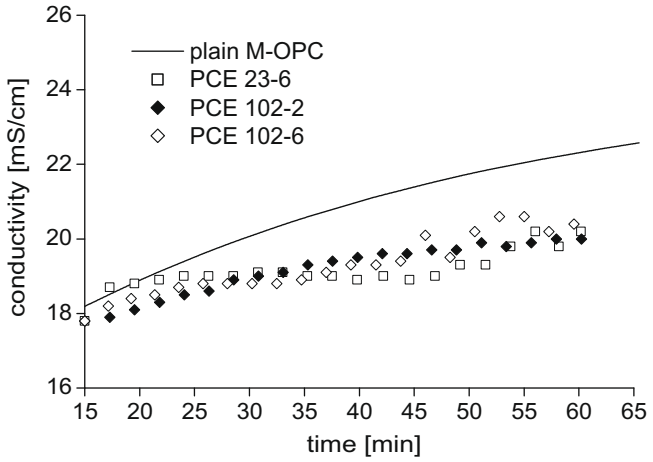

Fig. 8. Evolution of conductivities as a function of time of a plain M-OPC paste without PCE (line), with PCE 23-6, with PCE 102-2 and with PCE 102-6, respectively (symbols). All cement pastes were measured at a w/c of 0.35. The data collection started after 15 min. The conductivities are simultaneously recorded with the electroacoustic signals.

(Fig. 9) and reach saturation concentrations below 0.1 wt.-%. Despite similar adsorption isotherms (Fig. 7), the impact of side chain length on the zeta potential shows some C_3A-content dependency. PCE 102-6 reaches its saturation concentration in the L-OPC system faster than PCE 23-6. In the cement paste with medium C_3A-content (M-OPC) both PCE reach saturation at the same concentration whereas in the H-OPC, PCE 102-6 shows higher saturation concentration than PCE 23-6 does. This difference in C_3A-content dependency might be due to different adsorption rate which probably depends on the PCE architecture where on one hand the long side chained PCEs adsorb slower and on the other hand, the amount and dissolution rate of the C_3A may play a key role. In other words, the higher the amount of C_3A and the higher its reactivity, the more the interaction seems to be governed by the PCE adsorption rate. Another difference can be observed in the ability to shift the zeta potentials: both are close to zero, but PCE 23-6 stays negative whereas PCE 102-6 shows positive potentials. This is in agreement with findings of Plank et al. [5], where very long side chained PCE's are proved to change the negative into positive zeta potentials. This could be due to the fact that at same weight concentration, much more carboxylic groups are available with PCE 23-6. Furthermore, the amount of PCE 23-6 molecules is around four times higher than PCE 102-6 molecules for the same dosage by weight. Therefore, at same weight concentrations, PCE 23-6 covers a larger surface area and thus, a larger area is occupied with negative charged carboxyl groups.

PCE 102-2 reaches saturation concentration around 0.5 wt.-% in L-OPC and M-OPC cement pastes. At high C_3A-contents (H-OPC), saturation concentration is not yet reached at 0.5 wt.-%. However, according to TOC experiments, the molecules do hardly adsorb and thus, the adsorption data are in contrast to the zeta potential data. Two mechanisms could explain the data: (i) weak adsorption of the molecules (such as London forces, ion (particle surface) – dipole (PCE) bonds) on cement and hydrate particles, measurable with the ZetaProbe, but too weak to resist filtration-methods and (ii) strong influence of the PCE on the structural properties of the pore water (viscosity, surface tension, and cluster structure). The latter seem to be of major importance with increased molecular weight and dosage. In a cryo-microscopic study with the methods described in [18,44] could be observed that a large part of PCE 102-2 remains in the pore solution (unpublished results) and also strongly impacts the fracturing behaviour of the frozen sample. Up to now, the impact of PCE on the physical properties of the pore

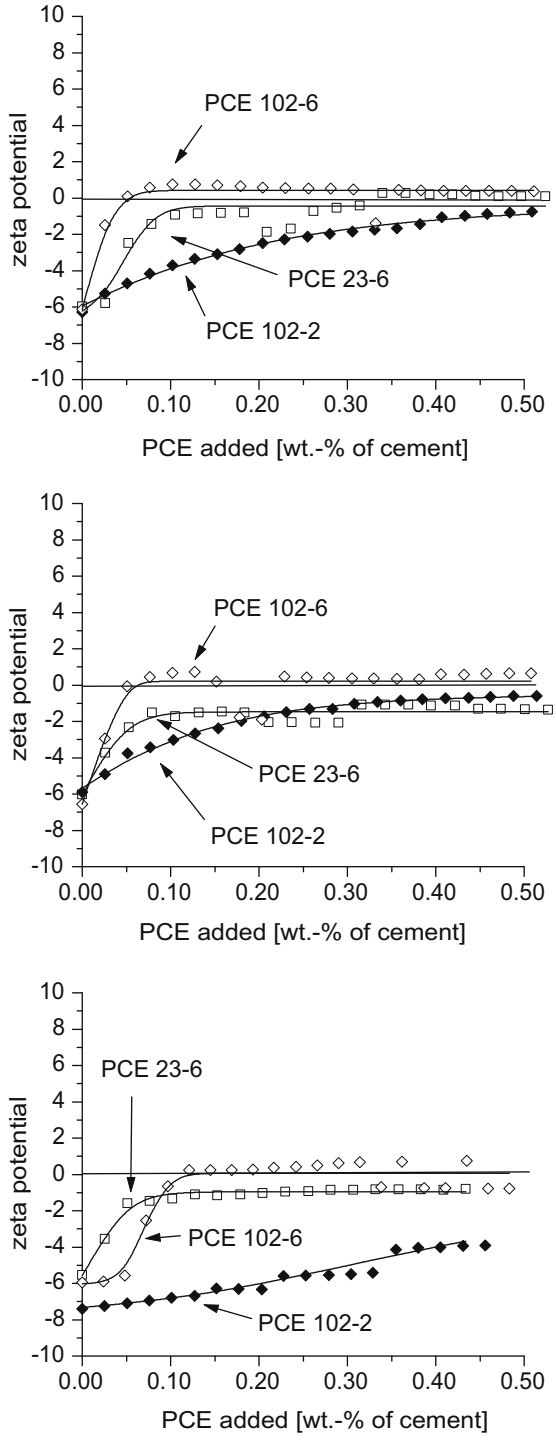

Fig. 9. Zeta potential curves of PCE titration experiments (increments of 0.025% weight of cement) on cement pastes with w/c 0.35 after 15 min of hydration. The C_3A-contents of the cements increase from top to bottom row. The data (symbols) were fitted (lines), the accuracy is ±1 mV.

solution is not very well investigated in the field of cement and concrete sciences.

5. Conclusions

In this parametric study, conduction calorimetry, rheology, adsorption isotherms, and zeta potential measurements were carried out in order to investigate the influence of PCE architecture and PCE dosage on cements containing different C_3A-contents.

In well balanced C_3A-sulphate CEM I type cements, containing a low to a medium C_3A-content, the influence of C_3A-content of the cement and the availability of sulphates on the performance of different cement–PCE couples (same concentrations) in terms of heat evolution and workability is relatively small. Generally, C_3A-contents require higher larger amounts of PCE in order to reach saturation concentration. Also, with increasing C_3A higher amounts of PCE are required to reach zero yield stress.

The calorimetry data shows that PCE with long side chains lead to significant smaller retardation times than PCE with short side chains. Consequently, the side chain length is the key parameter concerning the retardation effect of PCEs. At same weight concentration, approximately four times more PCE 23-6 molecules than PCE 102-2 and PCE 102-6 are added to the paste and are able to cover more surface area and thus, may act as a diffusion barrier.

This study shows that workability is mainly influenced by the ionic charge density of the PCE used. Therefore, the side chain density is the key parameter which controls the adsorption behaviour and thus the strength of electrostatic and steric stabilization. The latter governs the flow behaviour of the fresh cement pastes. It could be demonstrated, that the role of side chain length is of minor influence if PCE weight concentrations are compared. However, if the charge densities are taken in account, the PCE with higher PEO numbers in its side chains shows enhanced dispersion ability, which is due to its stronger steric repulsive forces. Despite the influence on the zeta potential of cement pastes, the very dense and long side chained PCE shows only minor impact on the paste rheology, which is supported by adsorption data.

From the obtained results and discussion, following hypothesis arise:

1. If not sufficient sulphate (or sulphate phases with lower dissolution rates) is available, anionic PCE molecules are alternatively adsorbed (competitive adsorption) in the diffuse double layer at the particle pore solution interface.
2. During the first hour of hydration, the increase of conductivity is lowered in presence of PCE. This indicates (weak) complexation, hindered dissolution by adsorbed PCE (acting as a diffusion barrier) or increased precipitation of hydrates. The latter might be a reason for early slump loss induced by some PCE–cement combinations.
3. A PCE with high side chain density and length (PCE 102-2) is weakly adsorbed onto surfaces by London forces or ion-dipole bonds. The weak PCE adsorption and its impact on the zeta potential can be measured. However, these bonds are too weak and the PCE molecules are removed with the pore solution during sample preparation for TOC analysis.
4. PCE molecules which remain in the pore solution have a significant impact on the physical properties of the pore solution such as water cluster structure, viscosity and surface tension. This might be of major importance for methods where those parameters significantly influence the measured data (e.g. zeta potential measurements).

These hypotheses require further studies of the superplasticizer interaction with pure clinker phases, hydrate phases and the pore solution. Furthermore, in terms of interparticle forces and associated rheological phenomena, the links to the microstructural evolution of a cement paste concerning particle size distribution, surface area and particle packing has to be investigated.

Acknowledgments

The authors would like to address their thanks especially BASF AG, Ludwigshafen (Germany) for the financial support of this study. We also would like to thank Luigi Brunetti, Heinz Gurtner,

Mélanie Miard and Oliver Nagel for their assistance during the laboratory experiments.

References

[1] Uchikawa H, Hanehara S, Sawaki D. The role of steric repulsive force in the dispersion of cement particles in fresh paste prepared with organic admixture. Cem Concr Res 1997;27(1):37–50.

[2] Kauppi A, Andersson KM, Bergström L. Probing the effect of superplasticizer adsorption on the surface forces using the colloidal probe AFM technique. Cem Concr Res 2005;35(1):133–40.

[3] Neubauer CM, Yang M, Jennings HM. Interparticle potential and sedimentation behaviour of cement suspensions: effects of admixtures. Adv Cem Based Mater 1998;8(1):17–27.

[4] Flatt RJ. Interparticle forces and superplasticizers in cement suspensions. EPFL, PhD thesis; 1999. p. 301.

[5] Plank J, Schwerd R, Vlad D, Brandl A, Chatziagorastou P. Kolloidchemische Aspekte zur Verflüssigung von Zementleimen mit Polycarboxylaten. In: Tagung Bauchemie. Monographie Bd., Erlangen, vol. 31; 2004. p. 58–69.

[6] Li C-Z, Feng N-Q, Li Y-D, Chen R-J. Effects of polyethlene oxide chains on the performance of polycarboxylate-type water-reducers. Cem Concr Res 2005;35(5):867–73.

[7] Hanehara S, Yamada K. Interaction between cement and chemical admixture from the point of cement hydration, adsorption behaviour of admixture, and paste rheology. Cem Concr Res 1999;29(8):1159–65.

[8] Yamada K, Takahashi T, Hanehara S, Matsuhisa M. Effects of the chemical structure on the properties of polycarboxylate-type superplasticizer. Cem Concr Res 2000;30(2):197–207.

[9] Kreppelt F, Weibel M, Zampini D, Romer M. Influence of solution chemistry on the hydration of polished clinker surfaces – a study of different types of polycarboxylic acid-based admixtures. Cem Concr Res 2002;32(2):187–98.

[10] Kirby GH, Lewis JA. Comb polymer architecture effects on the rheological property evolution of concentrated cement suspensions. J Am Ceram Soc 2004;87(9):1643–52.

[11] Cho H-Y, Suh J-M. Effects of the synthetic conditions of poly{carbosylate-g-(ethylene glycol) methyl ether} on the dispersibility in cement paste. Cem Concr Res 2005;35(5):891–9.

[12] Agarwal SK, Masood I, Malhotra SK. Compatibility of superplasticizers with different cements. Constr Build Mater 2000;14(5):253–9.

[13] Prince W, Espagne M, Aïtcin P-C. Ettringite formation: a crucial step in cement superplasticizer compatibility. Cem Concr Res 2003;33(5):635–41.

[14] Nikinamubanzi P-C, Aïtcin P-C. Cement and superplasticizer combinations: compatibility and robustness. Cem Concr Agg 2004;26(2):102–9.

[15] Winnefeld F, Becker S, Pakusch J, Gotz T. Effects of the molecular architecture of comb-shaped superplasticizers on their performance in cementitious systems. Cem Concr Compos 2007;29(4):251–62.

[16] Winnefeld F, Zingg A, Holzer L, Figi R, Pakusch J, Becker S. Interaction of polycarboxylate-based superplasticizers and Cements: influence of polymer structure and C_3A-content of cement. In: ICCC 2007. Montreal; 2007, CD: M6-03.2.

[17] Zingg A, Winnefeld F, Holzer L, Pakusch J, Becker S, Gauckler L. Adsorption of polyelectrolytes and its influence on the rheology, zeta potential, and microstructure of various cement and hydrate phases. J Colloids Interf Sci 2008;323(2):301–12.

[18] Zingg A, Gasser P, Winnefeld F, Kaech A, Pakusch J, Becker S, Holzer L. Cryo-microscopy for fresh cement pastes: first results. In: 8th CANMET/ACI International conference on superplasticizers and other chemical admixtures in concrete, vol. 2. Sorrento; 2006. p. 329–43.

[19] Zingg A, Holzer L, Kaech A, Winnefeld F, Pakusch J, Becker S, et al. The microstructure of dispersed and non-dispersed fresh cement pastes – new insight by cryo-microscopy. Cem Concr Res 2008;38(4):522–9.

[20] Locher FW, Richartz W, Sprung S. Setting of cement part II: effect of adding calcium sulphate. ZKG Int 1980;33(6):271–7.

[21] Lerch W. The influence of gypsum on the hydration and properties of Portland cement pastes 1946;46:1252–97.

[22] Lawrence CD. Physiochemical and mechanical properties of portland cements. In: Hewlett PC, editor. LEA'S chemistry of cement and concrete. Arnold: London; 1984. p. 343–420.

[23] Sandberg P. Optimization of cement sulfate part I: cement without admixture, in Application Notes. Application Notes Thermometric; 2004.

[24] Sandberg P. Optimization of cement sulfate part II: cement with admixture, in Application Notes. Application Notes Thermometric; 2004.

[25] Lothenbach B, Winnefeld F, Figi R. The influence of superplasticizers on the hydration of Portland cement. ICCC: Montreal, CD; 2007 [W1-05.3].

[26] Myrvold BO. Interactions between lignosulphonates and clinker minerals and the hydration products of clinker minerals. In: ICCC, Montreal, CD, vol. 1; 2007. p. M6-03.5.

[27] Plank J, Dai Z, Zouaoui N, Vlad D. Intercalation of polycarboxylate superplasticizers into C_3A hydrate phases. In: 8th CANMET/ACI international conference on superplasticizers and other chemical admixtures in concrete, Sorrento, vol. 2; 2006. p. 201–14.

[28] Flatt RJ, Houst YF. A simplified view on chemical effects perturbing the action of superplasticizers. Cem Concr Res 2001;31(8):1169–76.

[29] Peng J, Jindong Q, Zhang J, Chen M, Wan T. Adsorption characteristics of water-reducing agents on gypsum surface and its effect on the rheology of gypsum plaster. Cem Concr Res 2005;35(3):527–31.

[30] Yamada K, Ogawa S, Hanehara S. Controlling of the adsorption and dispersing force of polycarboxylate-type superplasticizer by sulfate ion concentration in aqueous phase. Cem Concr Res 2001;31(3):375–83.

[31] Plank J, Bassioni G, Dai Z, Keller H, Sachsenhauser B, Zouaoui N. Neues zur Wechselwirkung zwischen Zementen und Polycarboxylat-Fliessmitteln. In: 16. Internationale Baustofftagung, Weimar (D), vol. 1; 2006. p. 579–98.

[32] Vikan H, Justnes H, Winnefeld F, Figi R. Correlating cement characteristics with rheology of paste. Cem Concr Res 2007;37(11):1502–11.

[33] Plank J, Vlad D, Brandl A, Chatziagorastou P. Colloidal chemistry examination of the steric effect of polycarboxylate superplasticizers. Cem Int 2005;2005(3):100–10.

[34] Flatt RJ, Houst YF, Oesch R, Bowen P, Hofmann H, Widmer J, et al. Analysis of superplasticizers used in concrete. Anal Mag 1998;26(2):M 28–35.

[35] Yoshioka K, Tazawa E, Kawai K, Enohata T. Adsorption characteristics of superplasticizers on cement component minerals. Cem Concr Res 2002;32(10):1507–13.

[36] Uchikawa H. Function of organic admixture supporting high performance concrete. In: International RILEM conference PRO 5 function of organic admixture supporting high performance concrete; 1999. p. 69–97.

[37] Suzuki K, Nichikawa T, Kato K, Hayashi H, Ito S. Approach by zeta-potential measurement on the surface change of hydrating C_3S. Cem Concr Res 1981;11(5–6):759–64.

[38] Singh NB, Ojha PN. Changes in zeta potential during hydration of C_3S with and without $CaCl_2$ additions. J Am Ceram Soc 1981;64(7):C99.

[39] Naegele E, Ney P. A discussion of the paper "approach by zeta-potential measurement on the surface change of hydrating C_3S" K. Suzuki, T. Nichikawa, K. Kato, H. Hayashi, S. Ito. Cem Concr Res 1982;12(4):535–6.

[40] Houst YF, Flatt RJ, Bowen P, Hofmann H, Mäder U, Widmer J, et al. Optimization of superplasticizers: from research to application. In: International RILEM conference PRO 5 function of organic admixture supporting high performance concrete; 1999. p. 121–34.

[41] Naegele E. The zeta-potential of cement. Cem Concr Res 1985;15(3):453–62.

[42] Bjoernstroem J, Chandra S. Effect of superplasticizers on the rheological properties of cements. Mater Struct 2003;36(264):685–92.

[43] Richter F, Winkler EW. Das Calciumbindevermögen. Tenside Surfact Deter 1987;24(4):213–6.

[44] Holzer L, Gasser P, Kaech A, Wegmann M, Zingg A, Wepf R, et al. Cryo-FIB-nanotomography for quantitative analysis of particle structures in cement suspensions. J Microsc 2007;227(3):216–28.